Application Note

Cell Analysis

Agilent

Trusted Answers

Combining Live Cell Imaging with Cellular Impedance to Monitor Apoptotic Cell Death in Real Time

Authors

Jing Zhang, Nancy Li, Yama Abassi, and Brandon J. Lamarche
Agilent Technologies Inc.
San Diego, CA, USA

Grace Yang, Jiaming Zhang, and Peifang Ye
Agilent Biosciences Co. Ltd.
Hangzhou, China.

Introduction

Essential to diverse biological processes such as embryonic development and wound healing, apoptosis (also known as programmed cell death) is an evolutionarily conserved process that enables multicellular organisms to eliminate cells without triggering an inflammatory response. While defects in this cell clearance mechanism can give rise to cancer[1], overactive apoptosis plays a role in diseases such as lupus[2] and Parkinson's.[3] Once triggered by intrinsic or extrinsic stimuli, apoptosis causes a broad array of biochemical and morphological modifications ranging from cytoskeleton degradation and chromatin cleavage to protein cross-linking and phospholipid translocation.[4] The net result of these events is fragmentation of the cell into apoptotic bodies that are rapidly phagocytosed by macrophages.[5]

Although apoptosis can be tracked using various biomarker-based assays, these typically require multiple manual handling steps and only yield endpoint measurements. Requiring just a cell seeding step and a drug addition step, we used the Agilent xCELLigence RTCA eSight to continuously monitor drug-mediated apoptosis over the course of multiple days. Providing a direct and objective assessment of cell number, cell size, cell-substrate attachment strength, and cell barrier function, impedance biosensors embedded within the base of eSight microplates quantitatively track early (cell shrinkage) to late (fragmentation) apoptotic events with high analytical sensitivity. Concurrently, eSight captures live cell images in brightfield and three fluorescence channels (red, green, and blue), providing an orthogonal readout of the apoptosis process. By combining the strengths of real-time impedance monitoring (simplicity, analytical sensitivity, and objectivity) with that of live cell imaging (specificity of the readout), eSight increases the information richness of the apoptosis assay without increasing the workload. Importantly, the drug EC50 values determined using these two approaches are nearly identical, suggesting that eSight can simultaneously provide both the primary and secondary (confirmatory) readouts for apoptosis studies.

Assay principle

At the core of the eSight system is a specialized electronic microplate. Embedded within the glass bottom of all 96 wells, a gold biosensor array continuously and noninvasively monitors cellular impedance. As shown at the bottom of Figure 1, the adhesion of cells to these biosensors impedes the flow of a microampere electric current, providing a highly sensitive readout of cell number, cell size, cell-substrate attachment strength, and cell-cell interaction strength (that is, barrier function). This cellular impedance signal is recorded at a user-defined temporal resolution (every minute, once per hour), and is reported using a unitless parameter called Cell Index. The biochemical and cellular changes associated with apoptosis (cell shrinkage, detachment) are readily detected as a drop in the impedance signal. Positioned within the center of the biosensor array in each well, a viewing window enables eSight to also track cell health and behavior through live cell imaging in brightfield and three (red, green, blue) fluorescence channels (Figure 1). Agilent's companion reagents for eSight include lentiviruses for constructing cell lines that stably express nuclear-localized fluorescent proteins (red, green, blue), and dyes for visualizing live and dead cells (red, green). For apoptosis studies, Agilent has also developed annexin V reagents (coupled to red or green dyes) for visualization of translocated phosphatidylserine, and a reagent for visualizing caspase 3 activation. The latter consists of the canonical caspase 3 recognition motif, the DEVD tetrapeptide, linked to a green fluorogenic moiety. Although this membrane-permeable substrate is inherently nonfluorescent and does not bind to DNA, cleavage of the DEVD peptide releases the fluorophore, which can subsequently bind DNA and become fluorescent.

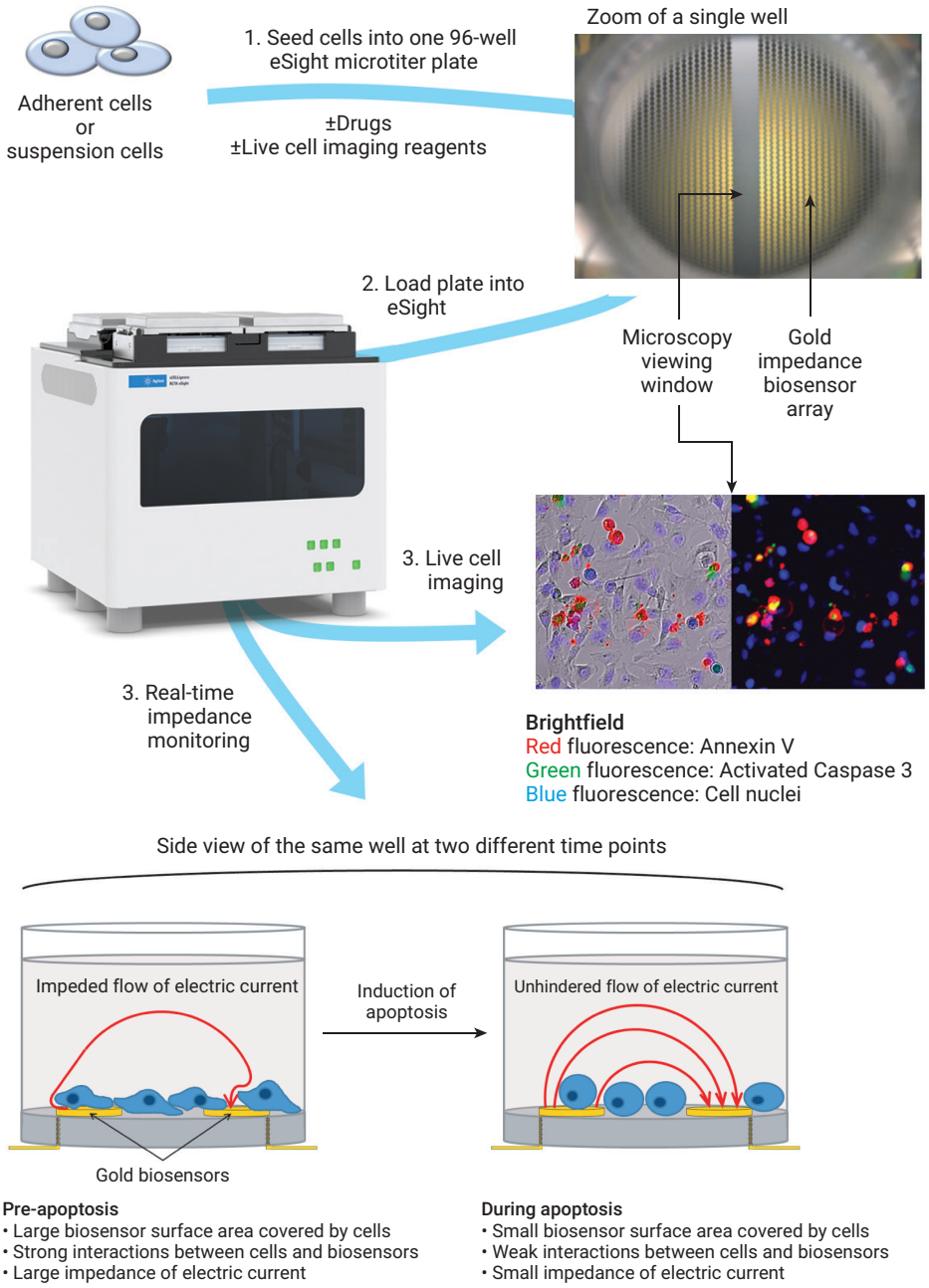

Figure 1. Agilent eSight workflow.

Materials and methods

Cell maintenance and assays were conducted at 37 °C/5% CO_2 in F-12K media (ATCC; catalog number 30-2004) containing 10% heat-inactivated FBS (Corning, catalog number 35016CV). While impedance was measured every 15 minutes, images were acquired once per hour. In each well, four fields of view were captured for each channel (brightfield, red, green, and blue). Exposure times were as follows: red (300 ms), green (300 ms), and blue (80 ms). The A549-Blue cell line, which stably expresses nuclear-localized blue fluorescent protein (BFP), was produced by transducing A549 cells (ATCC; catalog number CCL-185) with Agilent eLenti Blue (p/n 8711012) at a multiplicity of infection of 1. From day 2 to day 11 postinfection, 1 µg/mL puromycin was included in the growth medium to select for transductants. For real-time visualization of activated caspase 3, Agilent eCaspase 3 NucView 488 (p/n 8711005) was included in growth medium at a concentration of 5 µm. For real-time visualization of translocated phosphatidylserine, Agilent eAnnexin V Red (p/n 8711007) was included in growth medium at a concentration of 0.25 µg/mL. Agilent E-Plate VIEW microplates (p/n 00300601030) were also used. MG132 (Tocris; catalog number 1748/5) and staurosporine (Calbiochem; catalog number 569396) stocks were dissolved in DMSO.

Results

Multiplexing real-time impedance with live cell imaging to track cell killing

A549-Blue cells (described above) were seeded into an E-Plate VIEW at a density of 10,000 cells/well. As the cells proliferate over the first day, they occupy an expanding surface area on the biosensor array, causing the impedance signal to rise steadily (Figures 2A and 2B). If left untreated, the cells grow to confluence, saturating the biosensor array and giving a plateaued impedance signal. Addition of the proteasome inhibitor MG132 or the pan-kinase inhibitor staurosporine at the 25-hour time point induces a marked decrease in the impedance signal in a time- and dose-dependent manner.

The kinetics of these drug-induced responses, and the overall shape of the impedance traces, are distinct for each compound. This is consistent with a broad body of literature spanning over 10 years, which has demonstrated that impedance responses are typically unique for each type of mechanism of action.[6–8] Although MG132 and staurosporine both induce apoptosis,

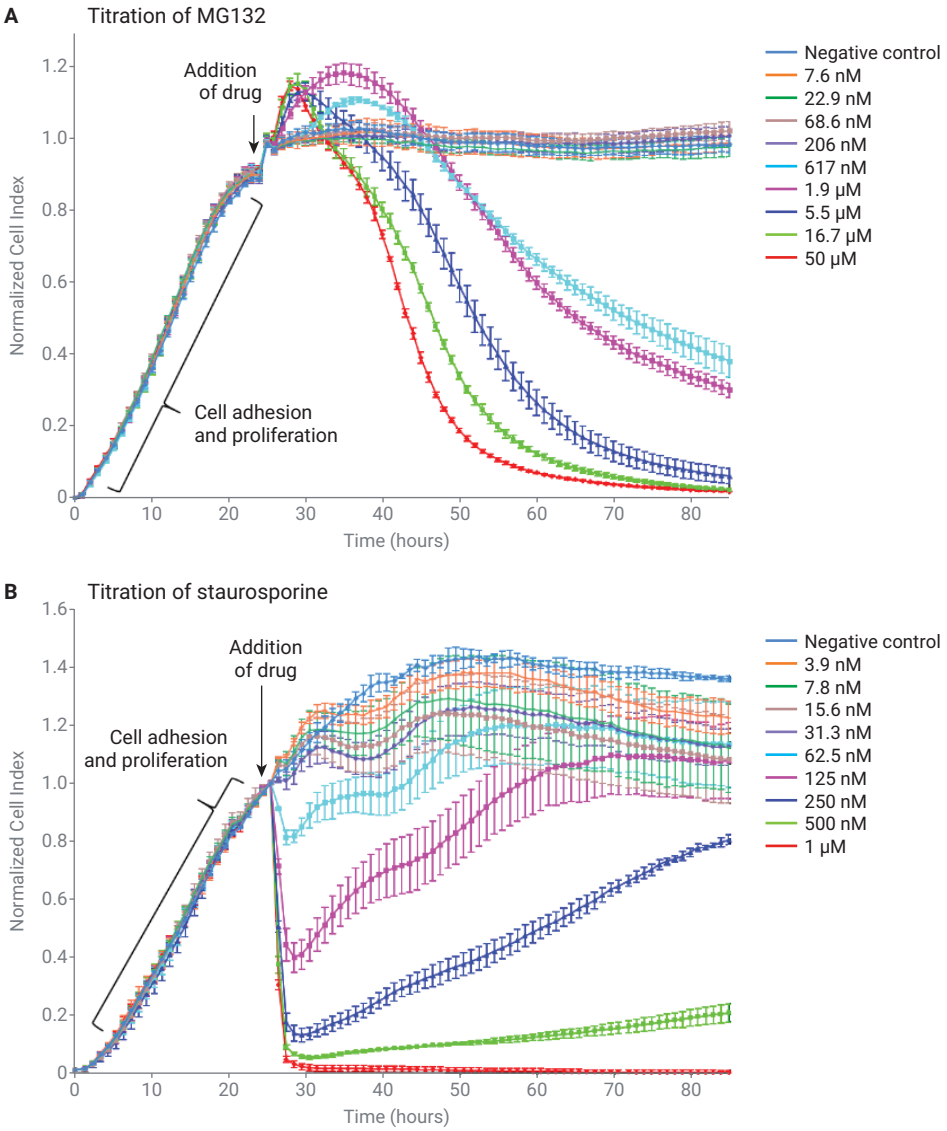

Figure 2. Tracking drug-induced apoptosis in real-time using cellular impedance. A549-Blue cells were titrated with either MG132 (A) or staurosporine (B). Negative control was DMSO. Error bars represent the standard deviation from samples run in triplicate. Although impedance was measured once every 15 minutes, to prevent the error bars from adjacent time points from overlapping, here data points are only shown once per hour.

they elicit distinct cellular behaviors en route to cell death, which becomes strikingly clear when real-time impedance is multiplexed with live cell imaging.

Although A549-Blue cells already cover most of the well bottom by the 26-hour time point, in the absence of drug, they continue proliferating for another 50 hours, packing cells together at higher density (Figure 3A). Consistent with this, the impedance signal plateaus at roughly 30 hours while the total number of blue nuclei continues to increase until ~80 hours (Figure 3A). When A549-Blue cells are treated with the four highest concentrations of MG132 (1.9, 5.5, 16.7, and 50 µm), the total number of blue nuclei decreases over time in a manner that correlates well with the drop in impedance (Figure 3B; only data for the 50 µm treatment are shown). In contrast, treating the cells with the four highest concentrations of staurosporine (0.125, 0.250, 0.500, and 1 µm) causes impedance to plummet within the first few minutes, but has a modest impact

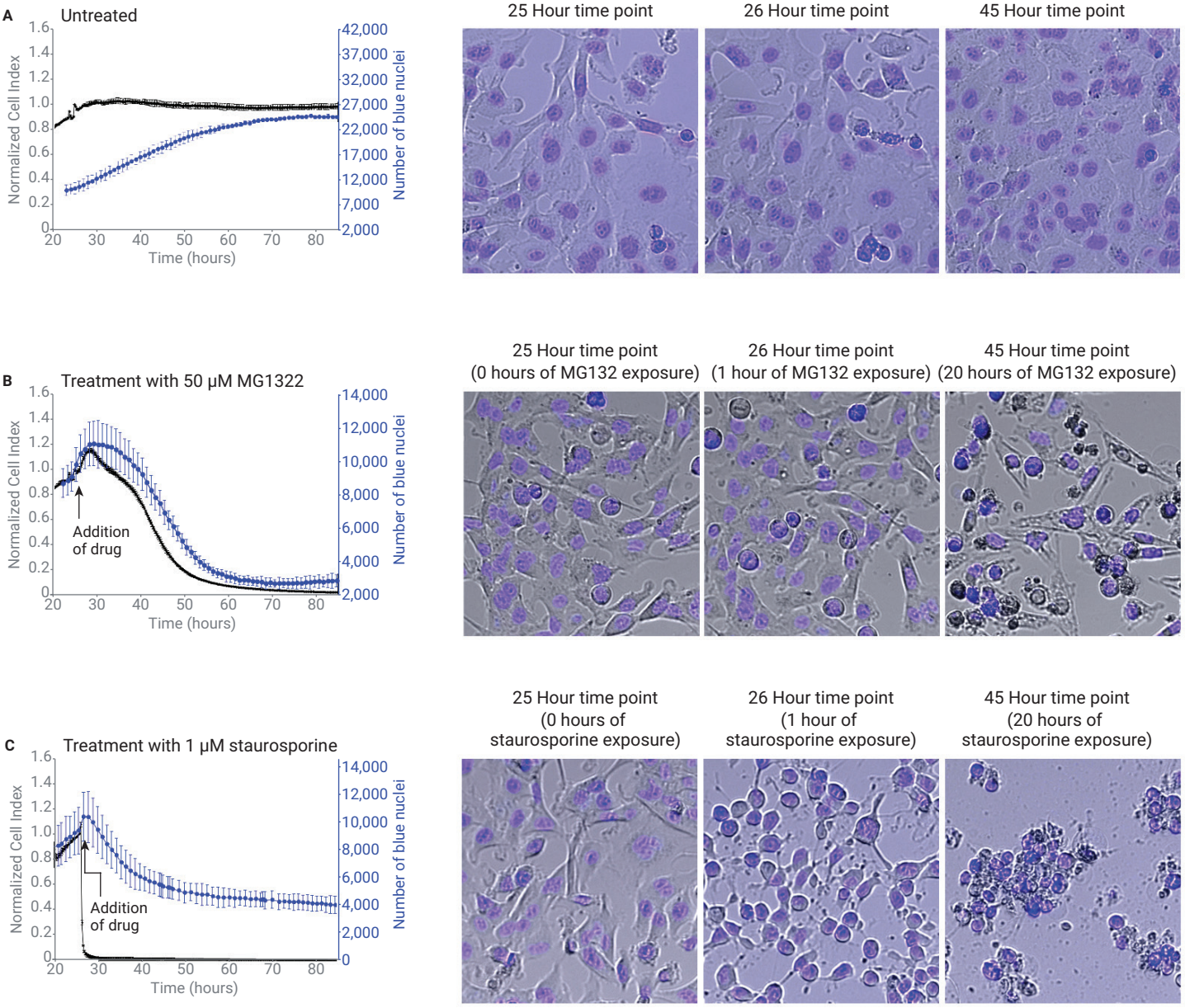

Figure 3. Correlating phenomena detected in real-time by impedance with specific cellular behaviors revealed by live cell imaging. The impedance signal and the number of blue nuclei were tracked after treating A549-Blue cells with either DMSO (untreated; A), 50 µm MG132 (B), or 1 µm staurosporine (C). Representative images are shown for pretreatment and 1 or 20 hours after treatment. Error bars represent the standard deviation from samples run in triplicate.

on the number of blue nuclei over the subsequent 60 hours (Figure 3C; only data for the 1 µm treatment are shown). Consistent with its ability to cause cells to expel water,[9] one hour after staurosporine addition, the A549-Blue cells have shrunk so severely that their cytoplasm is barely visible and only blue nuclei remain. Although, over time, these nuclei shrink in size and begin clustering together, they largely remain intact, explaining why the number of blue nuclei stays fairly constant in Figure 3C. The above coupling of impedance with imaging clearly provides a more complete and nuanced understanding of drug-mediated A549 cell killing than would be possible using either technique alone. Moving beyond simple cell counts, we next probed the kinetics of biochemical phenomena that are specific to the apoptotic killing pathway.

Simultaneously tracking MG132-mediated apoptosis from five different perspectives

Along with impedance and blue nuclei counts, the induction of apoptosis by MG132 was also tracked by percent cellular confluence, caspase 3 activation (causing cells to fluoresce green), and phosphatidylserine translocation (causing cells to fluoresce red). As seen in Figure 4, the drug-induced drop in impedance correlates well with the temporal accumulation of these apoptosis-specific markers. The bold white arrows in the panels for the 20- and 40-hour time points highlight large membrane blebs that contain phosphatidylserine in their outer leaflet.

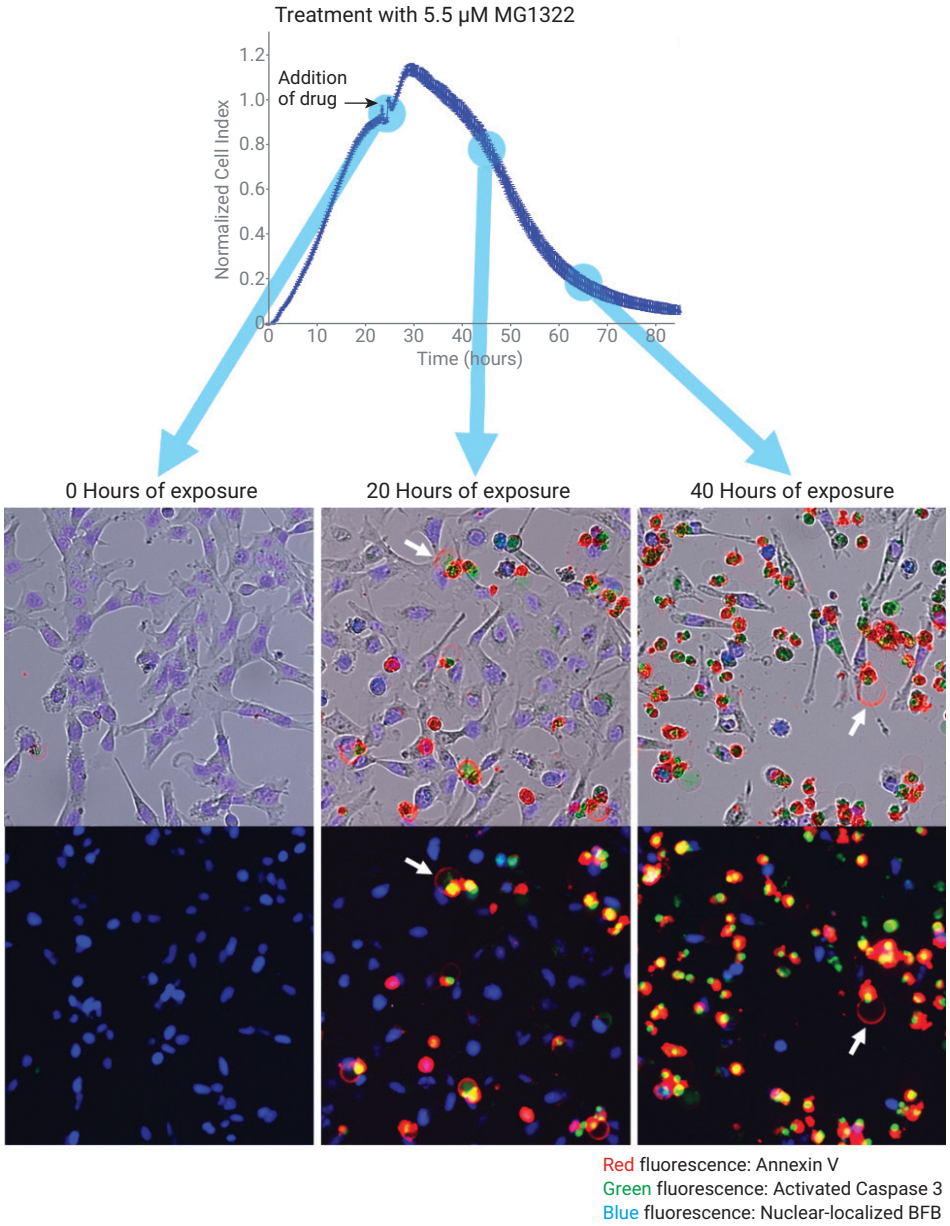

Figure 4. Corroborating the impedance response with live cell images. Image panels demonstrate the progression of apoptosis 20 and 40 hours after treating A549-Blue cells with 5.5 µm MG132. White arrows denote large membrane blebs that contain phosphatidylserine in their outer leaflet.

Next, the continuous response of A549-Blue cells to MG132 was plotted using each of the image-based readouts. Blue nuclei counts (Figure 5A) display a dependency on drug concentration that closely reflects the impedance responses seen in Figure 2A. Despite the extensive apoptotic response, throughout the course of this assay the % cellular confluence never drops below 50% (Figure 5B). This is consistent with the fact that, unlike *in vivo* contexts, where apoptotic cells and their debris are removed through phagocytosis, *in vitro*, a large percentage of apoptotic cells continue to occupy the well bottom (Figure 3B). The fact that high concentrations of MG132 cause the impedance signal to drop to zero (Figure 2A) while the % confluence never drops below 50% indicates that the residual cells are no longer attached to the plate bottom. The caspase 3 signal (Figure 5C) and the annexin V signal (Figure 5D) increase over time, and display clear dependencies on MG132 concentration. Considering the number of cells that were seeded, their rate of growth, and the percentage of cells that display apoptotic markers (Figure 4), the output numbers in Figure 5 are consistent with expectations.

To compare the relative rates and relative abundance of different apoptotic phenomena, the impedance response was plotted alongside three different image-based readouts (Figure 6). As expected, the time at which the number of blue nuclei begins to decrease (~10 hours after MG132 addition) is the same time that caspase 3 activation and phosphatidylserine translocation become detectable. For the first 20 hours of drug treatment, the number of cells displaying caspase 3 and phosphatidylserine signals is similar, but over the subsequent 40 hours, the number of caspase 3-activated cells exceeds the number of phosphatidylserine translocated cells by approximately 20%.

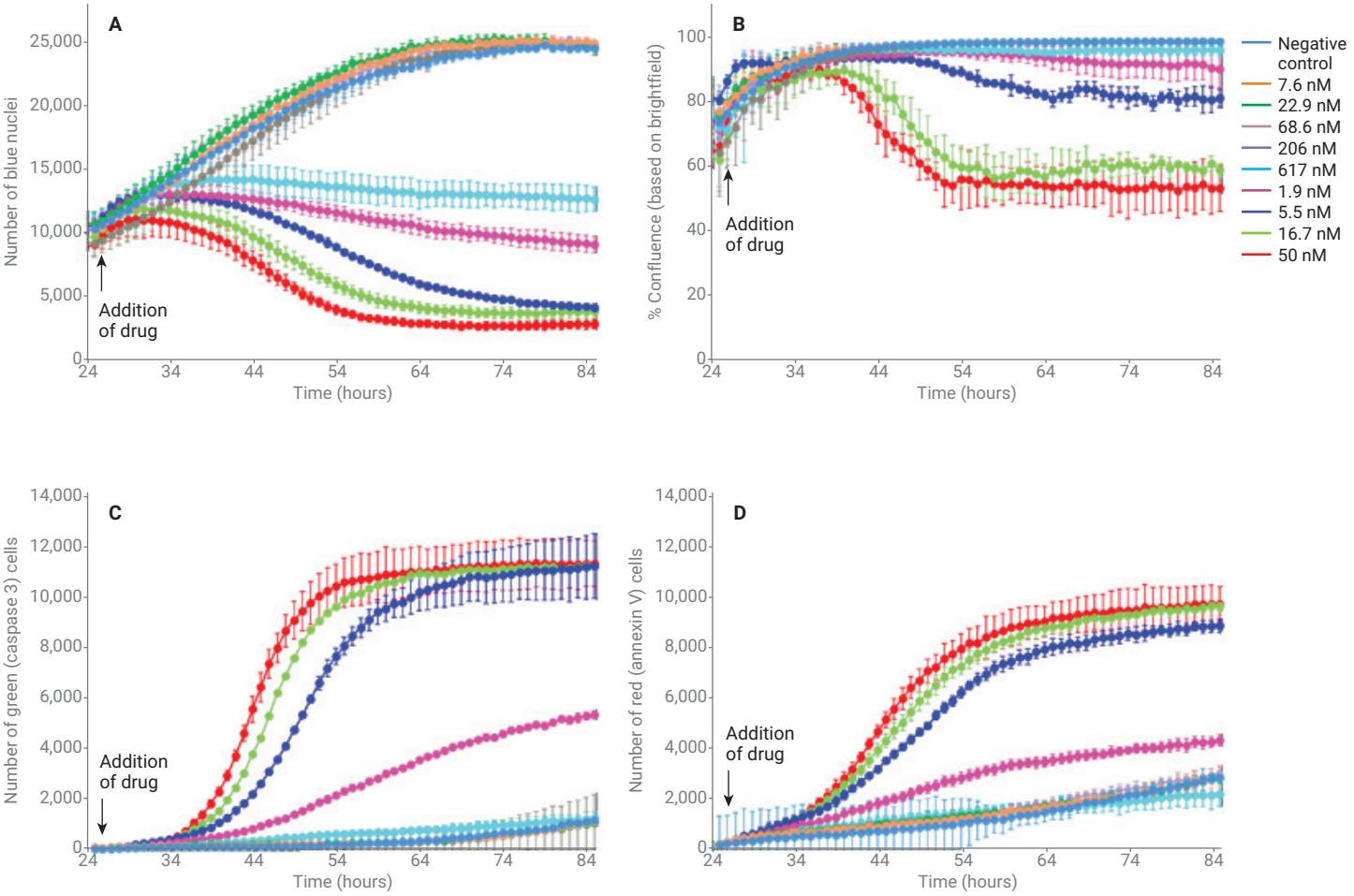

Figure 5. Image-based tracking of MG132-induced apoptosis in A549-Blue cells using number of blue nuclei (A), % confluence (B), number of green (caspase 3 activated) cells (C), and number of red (annexin V-bound) cells (D). Error bars represent the standard deviation from samples run in triplicate.

Quantifying drug efficacy

Using the impedance and image-based readouts presented in the previous sections, the EC50 for MG132 was calculated. The area under the curve, spanning from the time of drug addition to 60 hours after drug addition, was plotted as a function of MG132 concentration to yield the dose response curves seen in Figure 7. The quality of the fitting for the four different readouts is quite good, with R^2 values ranging from 0.96 to 0.98. The calculated EC50 values range from 0.86 to 3.0 µm, which is consistent with values reported in the literature.[10]

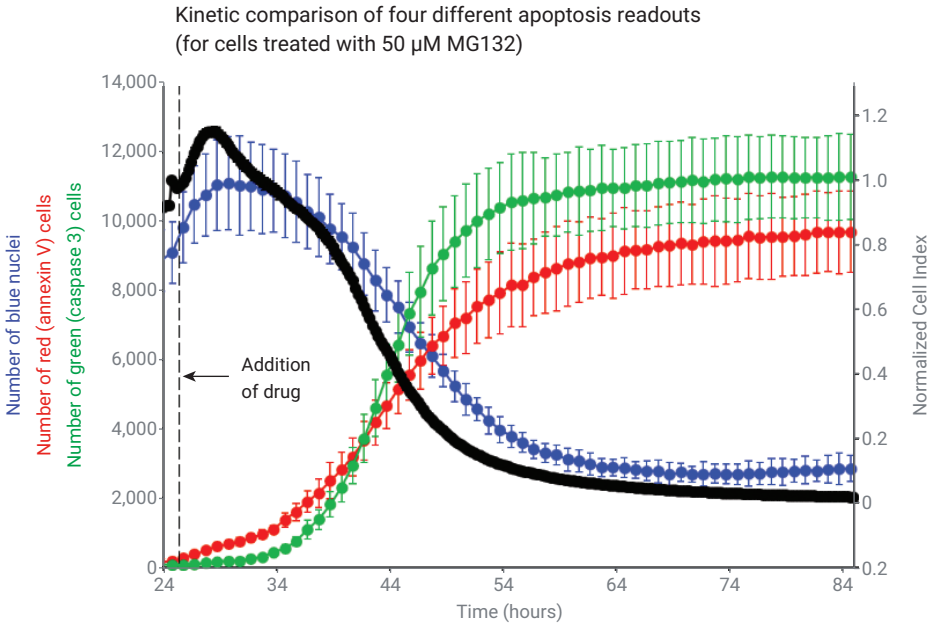

Figure 6. Comparing the relative rate and relative abundance of different apoptotic phenomena. Error bars represent the standard deviation from samples run in triplicate.

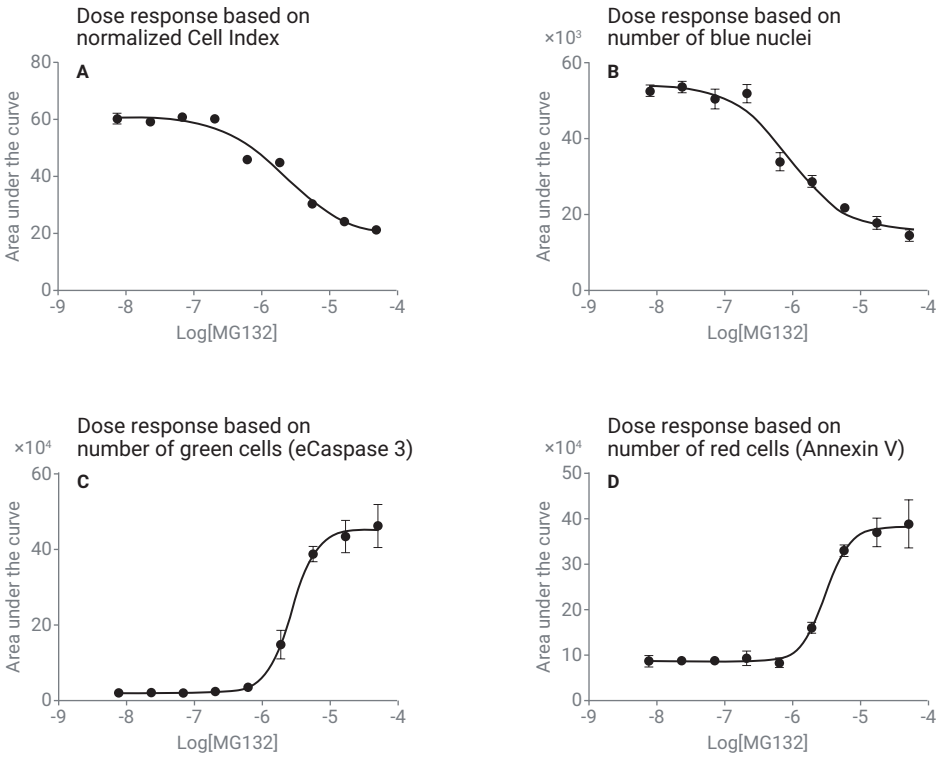

Parameter Analyzed	EC50 (µM)	R^2
Normalized Cell Index	2.3	0.97
Number of Blue Nuclei	0.86	0.96
Number of Green Cells (Capsase 3)	2.7	0.98
Number of Red Cells (Annexin V)	3.0	0.97

Figure 7. Dose response curves to calculate EC50. Using real-time impedance data (Figure 2A) and live cell imaging data (Figures 5A, 5C, and 5D), area under the curve was calculated, and is plotted here as a function of MG132 concentration. Data were fit to a four-parameter logistic equation to determine the EC50.

Conclusion

The power of multiplexing lies in the fact that it provides multiple vantage points for the question being addressed. The information richness of a multiplex assay lies not merely in the number of parameters it reports, but also in the distinctness/uniqueness of the perspectives that it affords. The xCELLigence RTCA eSight system enables cell health and behavior to be monitored simultaneously, and in the same well, from the very different perspectives of real-time cellular impedance and live cell imaging. It is the first instrument ever to combine these functionalities. The benefits of this dual readout are especially evident in Figures 2 and 3. Whereas impedance was able to detect a rapid staurosporine-mediated effect on A549-Blue cells, the cellular phenomena causing this change could not be deciphered using impedance alone. By revealing massive cytoplasmic shrinkage, live cell imaging immediately suggested a mechanistic explanation for the large and rapid impedance response. Impedance provided insights that would not have been obtainable by imaging alone. In one such example from the MG132 treatment, the impedance signal dropping to zero (Figure 2A) while cellular confluence remained >50% (Figure 5B) demonstrated that the cells still present in the well were completely detached. This ability to quantitatively assess cell-substrate attachment strength is unique to impedance.

The EC50 values calculated based on impedance (2.3 µm) and imaging (0.86 to 3.0 µm) are almost identical. Contributing to this consistency between the two data sets is the fact that both types of measurements are made on the exact same population of cells (that is, cells that are present in the same well). Such tight correlation of data from measurement techniques that are physically different provides a great deal of confidence in the conclusions being drawn, and suggests that eSight can serve as both the primary and secondary readout for apoptosis assays. Although the use of independent techniques to address a research question is universally considered to be best practice, this is often not done because it can greatly increase the amount of work required or the size of the sample that is needed. This is not the case with eSight assays, where every well provides a dual readout without any need for additional sample processing steps or increased sample size.

Beyond the benefit of having two independent measurement techniques, it is important to note the objectivity of the impedance readout, which is reported directly, without any processing or input from the user. Conversely, for eSight and all other imaging-based instruments, the raw image files get converted to outputs (such as number of blue nuclei) by user-informed algorithms where the expected size range, eccentricity, and brightness of cells must be defined. Although potential problems associated with this approach, such as inter-user variability, can be minimized through proper training and consistent usage of the same segmentation parameters, having impedance as an objective comparator helps build confidence in the assay's results.

While eSight can be used for a wide variety of toxicity assays, inclusion of Agilent eCaspase 3 and eAnnexin V reagents in the growth media endowed what would otherwise have been a general toxicity assay with apoptosis-specific readouts. Use of nuclear BFP-expressing cells provided the advantage of being able to count the total number of cells present, but this is not necessary as eCaspase 3 and eAnnexin V can be used on their own.

The continuous nature of the eSight assay has two major advantages. In contrast to endpoint assays that provide mere snapshots of a process, real-time tracking by eSight ensures that important phenomena do not get missed. Secondly, the continuous nature of eSight assays dramatically reduces that amount of hands-on time required to run an assay. Once cells have been seeded, and the apoptosis-effecting drug has been added, no further involvement is necessary.

In conclusion, the Agilent xCELLigence RTCA eSight apoptosis assay couples the simplicity, analytical sensitivity, and objectivity of real-time impedance monitoring with the highly specific readout of live cell imaging to continuously track this cell killing process with unparalleled information richness.

References

1. Yang, L. *et al.* Predominant Suppression of Apoptosome by Inhibitor of Apoptosis Protein in Non-Small Cell Lung Cancer H460 Cells: Therapeutic Effect of a Novel Polyarginine-Conjugated Smac Peptide. *Cancer Res*. **2003**, *63(4)*, 831–7.
2. Colonna, L.; Lood, C.; Elkon, K. B. Beyond Apoptosis in Lupus. *Curr. Opin. Rheumatol.* **2014**, *26(5)*, 459–66.
3. Venderova, K.; Park, D. S. Programmed Cell Death in Parkinson's Disease. *Cold Spring Harb. Perspect. Med*. **2012**, *2(8)*.
4. Elmore, S. Apoptosis: A Review of Programmed Cell Death. Toxicol. Pathol. 2007, 35(4), 495-516.
5. Nagata, S. Apoptosis and Clearance of Apoptotic Cells. *Annu. Rev. Immunol.* **2018**, *36*, 489-517.
6. Abassi, Y. A. *et al.* Kinetic Cell-Based Morphological Screening: Prediction of Mechanism of Compound Action and Off-Target Effects. *Chem. Biol.* **2009**, *16(7)*, 712–23.
7. Fu, H. *et al.* Kinetic Cellular Phenotypic Profiling: Prediction, Identification, and Analysis of Bioactive Natural Products. *Anal. Chem.* **2011**, *83(17)*, 6518–26.
8. Xing, J. Z. *et al.* Dynamic Monitoring of Cytotoxicity on Microelectronic Sensors. *Chem. Res. Toxicol.* **2005**, *18(2)*, 154–61.
9. Model, M. A. *et al.* Staurosporine-Induced Apoptotic Water Loss is Cell- and Attachment-Specific. *Apoptosis* **2018**, *23(7-8)*, 449–455.
10. Han, Y. H. *et al.* The Effect of MG132, a Proteasome Inhibitor on HeLa Cells in Relation to Cell Growth, Reactive Oxygen Species and GSH. *Oncol. Rep*. **2009**, *22(1)*, 215–21.

OLS OMNI Life Science GmbH
Germany, Austria +49 421 2761690
info@ols-bio.de | www.ols-bio.de
Switzerland freecall 0800 666 454
info@ols-bio.ch | www.ols-bio.ch

OLS® OMNI Life Science

www.agilent.com/chem/esight

For Research Use Only. Not for use in diagnostic procedures.

This information is subject to change without notice.

Printed in the USA, August 15, 2019
5994-1212EN

Agilent
Trusted Answers